Enhancement of the Madabhushi Liquid Jet in Crossflow Breakup Model by a Ligament Breakup Mechanism

Markus Lambert*[1], Thomas Esch[2], Markus Braun[1], Hossam Elasrag[3]
[1]ANSYS Germany GmbH,
Birkenweg 14a, 64295 Darmstadt, Germany
[2]ANSYS Germany GmbH
Staudenfeldweg 20, 83624 Otterfing, Germany
[3]ANSYS, Inc.
5930 Cornerstone Ct W San Diego, CA 92121, United States
*Markus Lambert: markus.lambert@ansys.com

Abstract
Liquid fuel jet atomization in a gaseous crossflow has been numerically simulated with the ANSYS Fluent CFD-Solver. The simulation utilized a Stress-Blended Eddy Simulation (SBES) model for turbulence closure [9] and the Discrete Particle Lagrangian Method (DPM) for the dispersed phase. For this purpose, the Madabhushi breakup model [1] was implemented into ANSYS Fluent. The original Madabhushi formulation was shown to overestimate the child droplet diameters after column breakup. An extension to the model is proposed here to overcome this limitation and to allow for a more realistic size distribution after initial ligament breakup. The new enhancement of the Madabhushi breakup model is compared to experimental data at different jet to air momentum flux ratios (J = 10, 20, We = 1500) provided by Gopola et al. [4] and Sekar et al. [5] and shows good agreement with measurement data.

Keywords
Atomizers, Liquid Jet in Crossflows (LJIC), Breakup Model, Droplet – Numerical

Introduction
The atomization of a liquid fuel jet in gaseous crossflows has many practical applications, like fuel injection in gas turbine engines, lean direct injectors (LDI) and lean premixed prevaporized ducts (LPP), as well as fuel injection in augmentors, scramjet and ramjet combustors. The atomization process can be divided into three regions [2]. The liquid column region where droplets are shed from the liquid core by surface wave mechanism, the column breakup region where the liquid core disintegrates into ligaments and large droplets and finally the spray region where the droplets undergo further breakup due to external aerodynamic forces. A schematic illustration of this complex process is shown in Figure 1(b).
The Madabhushi breakup model [1] is suitable for numerical simulations of liquid jets in subsonic crossflow. In this framework, the effects of primary breakup in the liquid core are simulated by the Wave breakup model [6], and the effects of ligament breakup after column breakup as well as the secondary breakup in the spray are simulated by a model suggested by Pilch and Erdman [3].
The original Madabhushi formulation has the tendency to overestimate the child droplet diameters after column breakup. A model extension by a ligament breakup mechanism is proposed that overcomes this limitation and allows for a more realistic size distribution after initial ligament breakup.
Results from the calculations are compared to experimental data at different jet to air momentum flux ratios (J = 10, 20, We = 1500) [4], [5] and show a good agreement with measurement data.
In the following sections we will describe the original Madabhushi formulation and our proposed extension. This will be followed by a description of the test cases and the used numerical settings. Finally, we will present and discuss the numerical results and the comparison with experimental data.
.

The Madabhushi breakup model and the proposed model extension
First, we give an overview over the Madabhushi breakup model and describe in detail the extension we propose and the basic idea. Figure 1(a) shows the particle breakup mechanism considered in the Madabhushi breakup model which will be described in some detail in the following section.

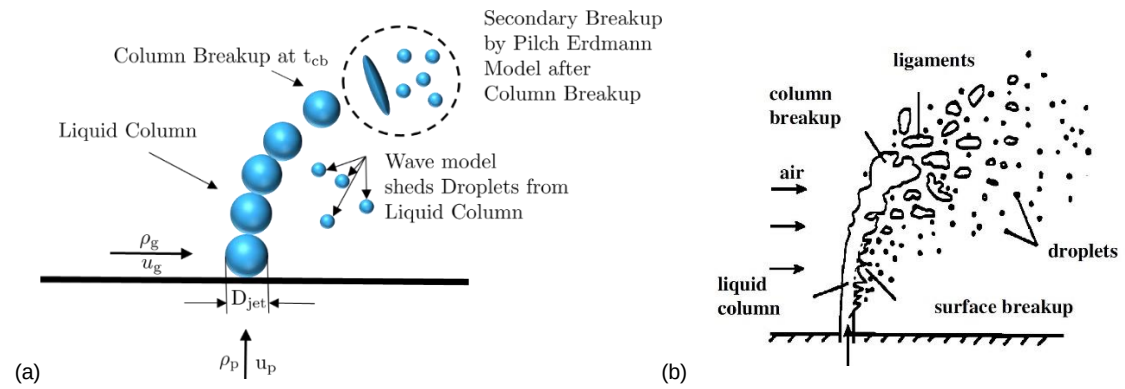

Figure 1. (a) Madabhushi breakup model, (b) Illustration of breakup of liquid jet in crossflow by Wu et al [2]

The droplets are injected through an orifice with an exit diameter D_{jet}. In the primary breakup stage, the jet is represented by spherical droplets of equal initial diameters $D_0 = D_{jet}$. The initial droplet velocity u_p is either known from the experiment or calculated from the liquid jet injection flow rate. During this phase, child droplets are shed according to the standard Wave breakup model [6]. Subsequent breakups (secondary breakup due to turbulence, capillary and aerodynamic forces) of these child droplets are modeled using the Pilch and Erdman model [3].
The droplets stay in the liquid column until the so-called column breakup time t_{cb} is reached:

$$t_{cb} = C_0 \frac{D_0}{u_g} \sqrt{\frac{\rho_l}{\rho_g}}, \quad C_0 = 3.44 \tag{1}$$

Here u_g is the magnitude of the gas velocity of the crossflow, ρ_l the liquid density, and ρ_g the gas density. C_0 is the column breakup time constant. Its value varies in different publications [7]. We use the value proposed in the work of Madabhushi [1] $C_0 = 3.44$. While the droplets are in the liquid column regime, the drag coefficient of the droplets remains constant at $C_D = 1.48$.
Once the droplet lifetime exceeds the column breakup time t_{cb}, it undergoes secondary breakup according to the Pilch and Erdman model [3]. The Pilch and Erdman model treats the breakup process in two stages. In the first stage, the droplet is deformed from a spherical shape to a disk shape within a deformation period t_{def}:

$$t_{def} = 1.6\, t^* \tag{2}$$

where t^* is the characteristic time scale given by:

$$t^* = \frac{D_{parent}}{u_{rel}} \sqrt{\frac{\rho_l}{\rho_g}} \tag{3}$$

u_{rel} is the magnitude of the slip velocity between droplet and gas, and D_{parent} is the local droplet diameter at the start of the breakup process. During the deformation period, the droplet's drag changes due to the change in droplet shape and droplet cross sectional area. The second stage starts after the deformation time, t_{def}, is reached. The droplet remains in a disc shape and the drag coefficient stays constant with a value of $C_D^{disc} = 1.2$ until the droplet breaks up into several smaller child droplets. The total breakup time, t_b, is dependent on the local Weber number and the characteristic time scale t^* [1], [3]. Depending on the local Weber number, droplet breakup may occur continuously between t_{def} and t_b (We > 40) or mostly during the second half of the time interval (We < 40). Upon breakup the child droplets inherit the parent droplet velocity, $\vec{u}_{parent}$, plus a velocity component due to the rim expansion of the parent droplet, $\vec{u}_n$.:

$$\vec{u}_{child} = \vec{u}_{parent} + \vec{u}_n \tag{4}$$

$\vec{u}_n$ lies in a plane normal to the parent droplet velocity as shown in Figure 2; its magnitude is expressed as:

$$u_n = 5 \frac{D_{parent}}{t_b - t_{def}} \tag{5}$$

For each of the droplets, the normal velocity direction angle α is randomly chosen in the range [0,2π].

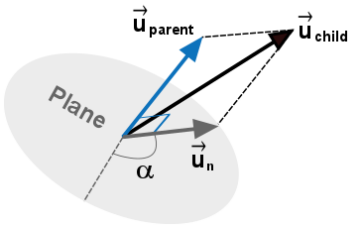

Figure 2. Child Droplet Velocity

The target volumetric distribution of child droplets after breakup is given by the following root-normal distribution [8]:

$$f(D_{child}) = \frac{\sqrt{\frac{D_{child}}{D_{0.5}}}}{2\sqrt{2\pi}\ 0.238\ D_{child}}\ exp\left(-\frac{1}{2}\left(\frac{\sqrt{\frac{D_{child}}{D_{0.5}}}-1}{0.238}\right)^2\right) \tag{6}$$

where $D_{0.5} = 1.2\ D_{SMD}$ is the mass median diameter related to the target Sauter mean diameter after breakup as:

$$D_{SMD} = 1.5\frac{Oh^{0.2}}{We_{corr}^{0.25}}D_{parent} \tag{7}$$

Oh is the Ohnesorge number given by:

$$Oh = \frac{\mu_l}{\sqrt{\rho_l D_{ref}\sigma_l}} \tag{8}$$

Here, μ_l is the droplet viscosity, σ_l is the droplet surface tension, and D_{ref} is the reference diameter of the deformed droplet given by:

$$D_{ref} = \begin{cases} \left(1 + 0.19\sqrt{We}\right)D_{parent} & ,We < 100 \\ 2.9\ D_{parent} & ,We \geq 100 \end{cases} \tag{9}$$

We_{corr} is the Weber number corrected for high droplet viscosity (Oh > 0.1). It is calculated as:

$$We_{corr} = \frac{We}{1 + 1.077\ Oh^{1.6}} \tag{10}$$

The droplets that undergo secondary breakup after column breakup represent real-world ligaments breaking up from the liquid core. The ligaments vary in shape and eventually break into smaller ligaments that are not equal in size to the original child droplets produced by the Pilch and Erdman model, which assumes almost spherical parent droplets. The Pilch and Erdman model has the tendency to overestimate the child droplet diameters in this region. Figure 3 illustrates this tendency. It shows the numerically calculated Sauter mean diameter at the center line of the measurement plane at 30 jet diameters downstream of the jet inlet compared to experimental data provided by Sekar et al. [5].
To overcome this inaccuracy, we propose the following enhancement to the original formulation of Madabhushi [1]. The diameters of the child droplets that are created immediately after column breakup must be weighted by a factor $F_{Lig} > 0$ to consider the influence of ligaments:

$$D_{child} = F_{Lig}\overline{D}_{child} \tag{11}$$

$\overline{D}_{child}$ follows the same target volumetric distribution as shown in Equation (6). After this step, the child droplets continue to break up further according to the original Pilch and Erdman model; i.e. with no child droplet diameter weighting (that is $F_{Lig} = 1$) until they become so small that the surface tension prevents further breakup.
Figure 3 shows the improvement of the results using a child droplet diameter weight of $F_{Lig} = 0.4$ compared to the original Madabhushi breakup model ($F_{Lig} = 1$).

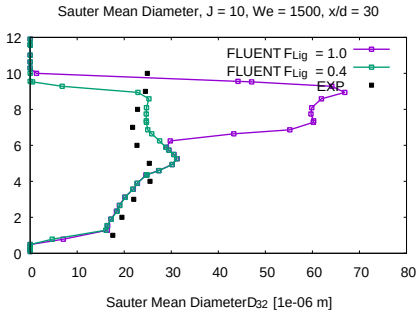

Figure 3. Original Madabhushi breakup model $F_{Lig} = 1$ vs. new approach $F_{Lig} = 0.4$

Test Conditions

A detailed description of the experimental setup and the test facility used for the model validation can be found in Gopola et al. [4]. We compare our numerical results with the experimental data of two test cases with different jet to air momentum flux ratios $J = \frac{\rho_l {u_l}^2}{\rho_g {u_g}^2}$ of $J = 10$ and $J = 20$ provided in Sekar et al. [5]. Figure 4 shows a sketch of the used simulation setup. The rectangular test section has a length of 0.06858 m (l/d ~ 150) and a quadratic cross section of width 0.04318 m (w/d ~ 95). The injector under investigation has a diameter of 457 micron and is placed on the centreline of the lower wall 0.02 m from the air inlet. Jet-A fuel is injected into the crossflowing air. The gas temperature is set to 300K and the pressure to a value of 506625 Pa. The air velocity magnitude is chosen in that way that an injection Weber number of 1500 is achieved for either of the two jet to air momentum flux ratios of 10 and 20.

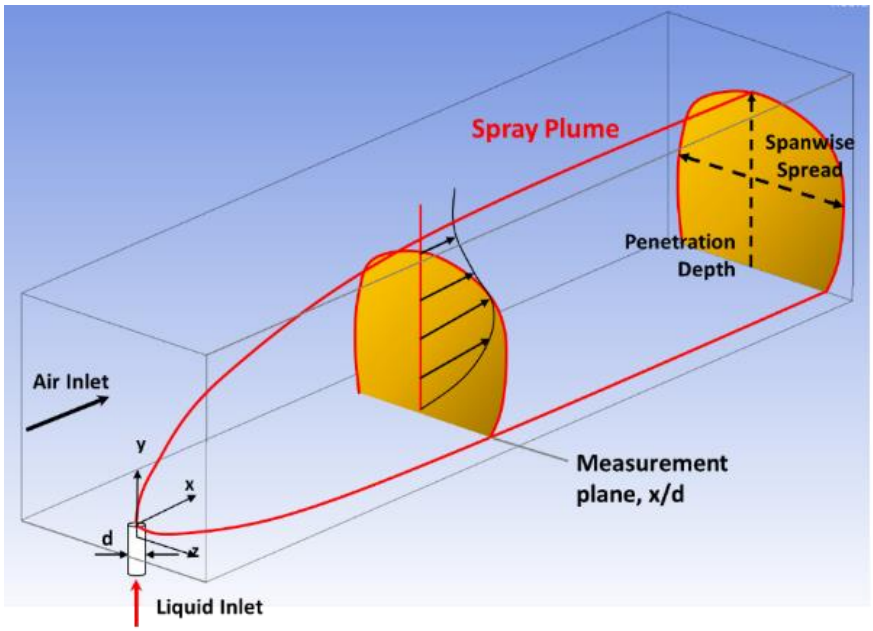

Figure 4. Liquid jet in Crossflow Sketch of Spray and Definitions

Results and discussion

A schematic view of the mesh at the midplane section of the computational domain is shown in Figure 5. A polyhedral mesh with approximately 3.2 million cells is used with a near wall boundary layer resolution of $y^+ \sim 1$ and a mesh refinement around the jet inlet area. The red lines mark the positions of the measurement planes at x/d = 30 and x/d = 60 jet diameters downstream from the jet inlet. The comparison with the experimental data provided by Sekar et al. [5] is done in those two planes.

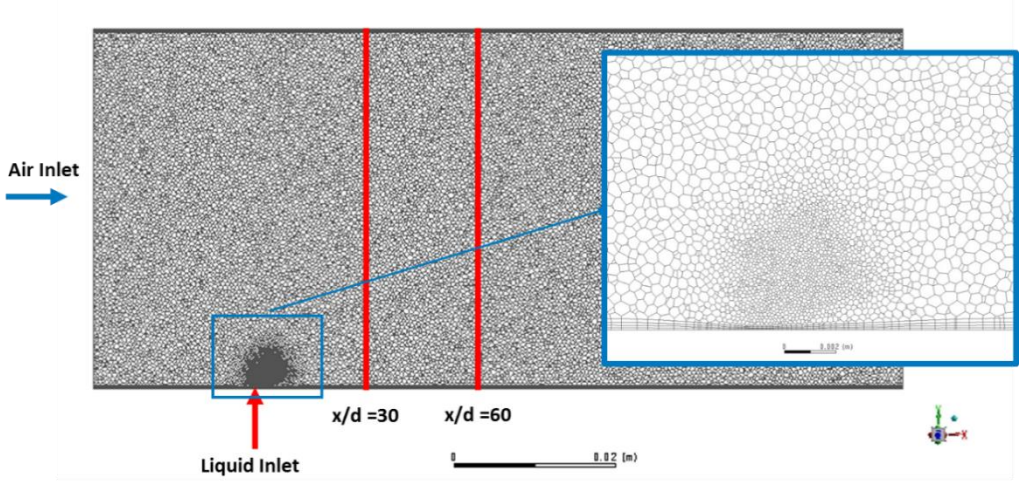

Figure 5. Polyhedral mesh ca. 3.2 million cells, near wall boundary layer resolution $y^+ \sim 1$, midplane cut, mesh refinement around jet inlet area, red lines: measurement planes at x/d = 30 and x/d = 60

For the CFD predictions ANSYS Fluent is used to resolve the complex and transient flow system around the jet inlet using a Stress-Blended Eddy Simulation (SBES) [9] with k-ω SST turbulence model and the dynamic Smagorinsky subscale model. The Discrete Particle Method (DPM) is used to simulate the droplet behaviour and is two way coupled with the flow. As droplet breakup model the enhanced Madabhushi breakup model with a ligament factor $F_{Lig} = 0.4$, Wave model constants $B_1 = 10$, $B_0 = 2.44$ and column breakup time constant $C_0 = 3.44$ is used. Particles are injected using a solid cone injection with a half cone-angle of $10°$. On average there are 35,000 computational droplets in the simulation domain. After an initial phase of 0.01s simulated physical time to reach the fully developed free channel air flow state, droplets are injected for the first time. After another period of 0.01s simulated physical time where the jet-air-crossflow system reaches a quasi-stationary state, droplet sampling at the experimental measurement planes is started. During a final third simulation period the Sauter mean diameter and the mean droplet x-velocity are averaged over a physical period of 0.01s; during this time on average 10 full droplet cycles from injection to outflow cross the measurement planes i.e. the statistical data are based on about 350,000 events.

Figure 6 and Figure 7 show the Sauter mean diameter (SMD) as well as the mean droplet x-velocity at the midline of the measurement planes at x/d = 30 and x/d = 60 downstream of the injector for the first test case (We = 1500 and J = 10). At both locations we are in good agreement with the experimental data considering the penetration length and the near wall droplet diameter distribution as well as the droplet diameter distribution close to the spray upper edge. The droplet diameter is slightly overestimated at 5 to 8 mm above the wall at x/d = 30 and 5 to 9 mm above the wall at x/d = 60 respectively. The mean droplet x-velocity is slightly overestimated in the near wall region and slightly underestimated close to spray edge. Overall both quantities, SMD and mean droplet x-velocity, are in good agreement with the experimental data.

The spanwise spread of the spray is under predicted at both locations x/d = 30 and x/d = 60 as shown in Figures 10 and 11. Beside the spanwise spread of droplets the Sauter mean diameter distribution is in good agreement with the experimental data in both measurement planes. The main characteristics of the Sauter mean diameter distribution in the spray are captured.

Similar results have been obtained for the test case with a higher jet to air momentum flux ratio of J = 20 as shown in Figure 8 and Figure 9. Due to lack of experimental data, we can only present the comparison along the centerline of the measurement planes at x/d = 30 and x/d = 60. Like for the case with the smaller jet to air momentum flux ratio, at both locations we are in good agreement with the experimental data considering the penetration length and the diameter distributions close to the wall as well as close to the spray edge. In a small region in between the spray limits the mean droplet diameter is slightly overestimated. For the mean droplet x-velocity the simulation data are in good agreement with the experimental data.

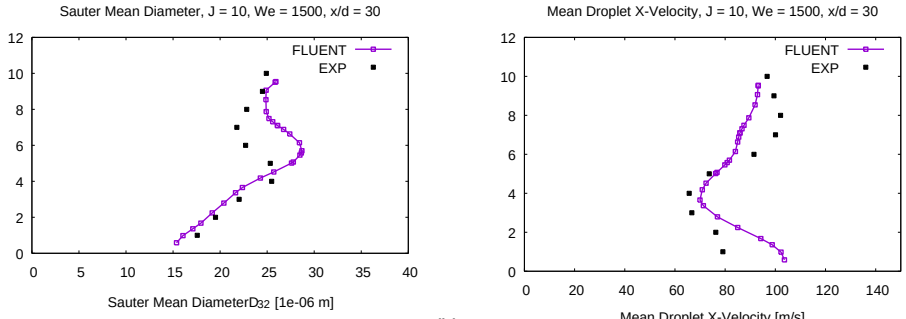

(a) (b)

Figure 6. (a) Sauter Mean Diameter (b) Mean Droplet X-Velocity at 30 jet diameters downstream respectively as a function of y-coordinate using model parameter B1 = 10, B0 = 2.44, $C_0 = 3.44$, $F_{Lig} = 0.4$, for We = 1500, J = 10 test case

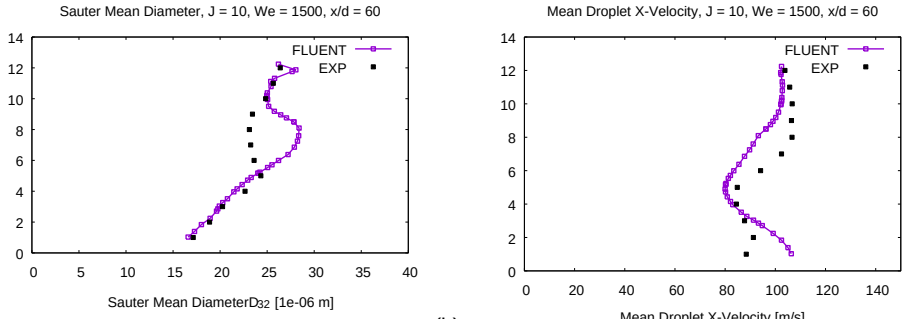

(a) (b)

Figure 7. (a) Sauter Mean Diameter (b) Mean Droplet X-Velocity at 60 jet diameters downstream respectively as a function of y-coordinate using model parameter B1 = 10, B0 = 2.44, $C_0 = 3.44$, $F_{Lig} = 0.4$, for We = 1500, J = 10 test case

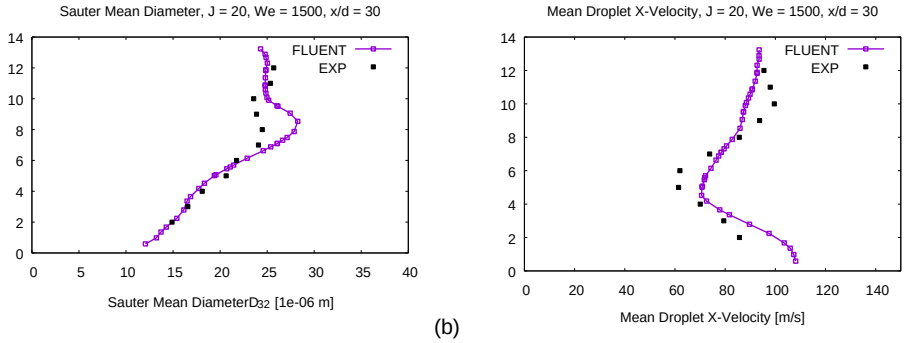

(a) (b)

Figure 8. (a) Sauter Mean Diameter (b) Mean Droplet X-Velocity at 30 jet diameters downstream respectively as a function of y-coordinate using model parameter B1 = 10, B0 = 2.44, $C_0 = 3.44$, $F_{Lig} = 0.4$, for We = 1500, J = 20 test case

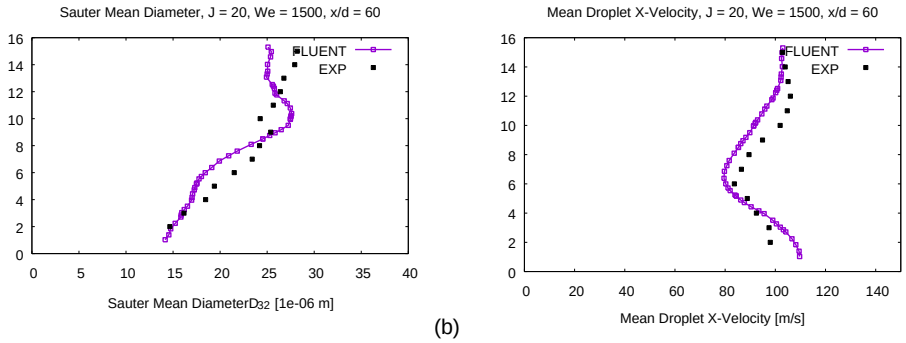

(a) (b)

Figure 9. (a) Sauter Mean Diameter (b) Mean Droplet X-Velocity at 60 jet diameters downstream respectively as a function of y-coordinate using model parameter B1 = 10, B0 = 2.44, $C_0 = 3.44$, $F_{Lig} = 0.4$, for We = 1500, J = 20 test case

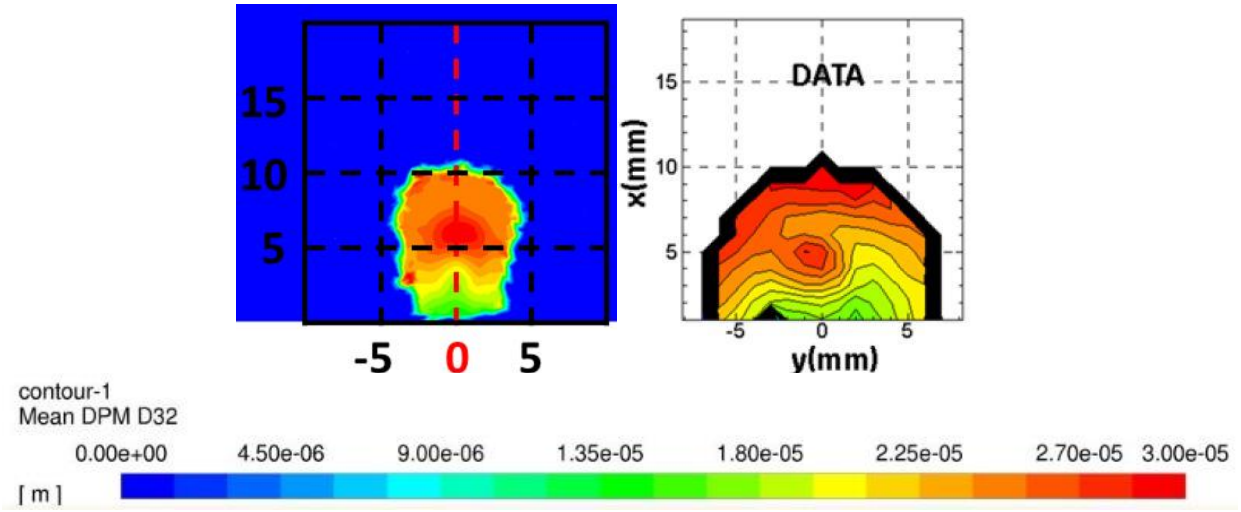

(a) (b)

Figure 10. Sauter Mean Diameter (a) FLUENT simulation (b) Experimental Data Sekar et al. [5] at 30 jet diameters downstream respectively using model parameter B1 = 10, B0 = 2.44, C0 = 3.44, $F_{Lig} = 0.4$, for We = 1500, J = 10 test case

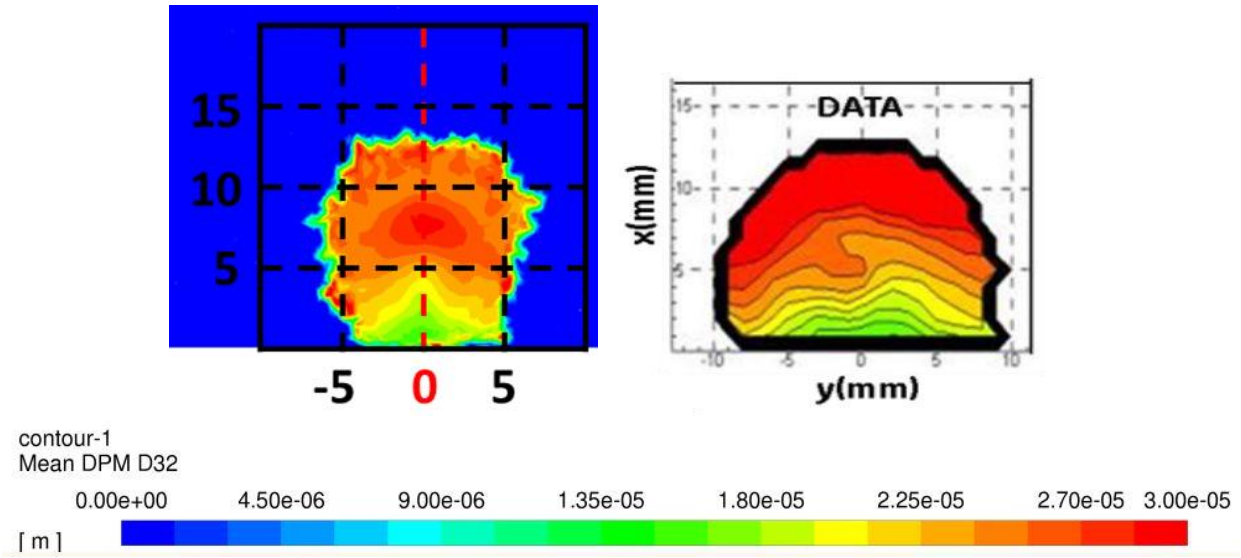

(a) (b)

Figure 11. Sauter Mean Diameter (a) FLUENT simulation (b) Experimental Data Sekar et al. [5] at 60 jet diameters downstream respectively using model parameter B1 = 10, B0 = 2.44, C0 = 3.44, $F_{Lig} = 0.4$, for We = 1500, J = 10 test case

Conclusions

The atomization of a liquid fuel jet in a gaseous crossflow in a rectangular test section has been simulated with the ANSYS Fluent CFD solver using a Stress-Blended Eddy Simulation (SBES) [9] with k-ω SST turbulence model and dynamic Smagorinsky subscale model; two way coupled with the Discrete Particle Method. A model extension of the Madabhushi breakup model [1] was proposed that overcomes the limitation of overestimating the child droplet diameters after column breakup and allows for a more realistic size distribution after initial ligament breakup. The model extension was validated comparing the numerical results to experimental data at different jet to air momentum flux ratios (J = 10, 20, We = 1500) provided by Gopola et al. [4] and Sekar et al. [5] and showed good agreement with measurement data. Parameter studies varying the breakup model parameters to calibrate the model were done but not presented in this paper. The extended Madabhushi breakup model works well for different jet to air momentum flux ratios. The spanwise spread of the spray is underpredicted. It is assumed that this might be due to not capturing the wake region behind the jet by CFD in conjunction with DPM. In the future simulations are planned to investigate the impact of the flow blockage due to the liquid jet column on the spanwise spread of the spray plume downstream of the injector. Further investigations of the characteristics of the breakup process will follow using the new hybrid multiphase model "VOF-to-DPM" in Fluent [11]. These steps may give more insight into

the physical mechanisms of the breakup process and may allow for an improvement of the semi-empirical breakup models that are currently used in large scale technical applications.

Nomenclature

C_0	column breakup time constant
D_{Jet}	jet diameter [m]
D_{parent}	diameter of parent droplet in breakup [m]
D_{child}	diameter of child droplet in breakup [m]
$D_{0.5}$	mass median diameter [m]
D_{SMD}	Sauter mean diameter [m]
D_{ref}	reference area of the deformed droplet [m]
D_0	initial diameter of injected droplets [m]
J	jet to air momentum flux ratio $J = \rho_l {u_l}^2 / \rho_g {u_g}^2$
Oh	local Ohnesorge number $Oh = \mu_l / \sqrt{\rho_l D_{ref} \sigma_l}$
ρ_l	density liquid $[kg/m^3]$
ρ_g	density gas $[kg/m^3]$
t_{def}	deformation time period [s]
t_b	total breakup time [s]
t^*	characteristic time scale for breakup [s]
t_{cb}	column breakup time [s]
u_g	magnitude of the gas velocity of the crossflow $[m/s]$
u_{rel}	magnitude of the relative velocity between droplet and gas $[m/s]$
$\vec{u}_{\mathrm{child}}$	velocity of child droplet $[m/s]$
$\vec{u}_{\mathrm{parent}}$	velocity of parent droplet $[m/s]$
$\vec{u}_{\mathrm{n}}$	normal velocity in a plane normal to the parent droplet velocity $[m/s]$
u_n	magnitude of the normal velocity in a plane normal to the parent droplet velocity $[m/s]$
We	local Weber number $We = \rho_g u_{rel}^2 D_{parent} / \sigma_l$
We_{corr}	Weber number for high droplet viscosity (Oh > 0.1)

References

[1] Madabhushi, R. K., “A Model for Numerical Simulation of Breakup of a Liquid Jet in Crossflow”, 2003, Atomization and Sprays, vol. 13, pp. 413-424.
[2] Wu, P. K., Kirkendall, K. A. and Fuller, R. P., “Breakup Processes of Liquid Jets in Subsonic Crossflow”, 1997, J. Propulsion and Power, vol. 13, pp. 64-73.
[3] Pilch, M. and Erdman, C. A., “Use of Breakup Time Data and Velocity History Data to Predict the Maximum Size of Stable Fragments for Acceleration-Induced Breakup of a Liquid Drop”, 1987, Int. J. Multiphase Flow, vol. 13, pp. 741–757.
[4] Gopala, Y., Zhang, P., Bibik, O., Lubarsky, E., Zinn, B. T., “Liquid Jet in Crossflow – Trajectory Correlations based on the Column Breakup Point”, 2010, AIAA 2010-214, 48th AIAA Aerospace Sciences Meeting, Florida, USA.
[5] Sekar, J., Rao, A., Pillutla, S., Danis, A. and Hsieh, S.Y., “Liquid Jet in Cross Flow Modeling”, June 16 – 20, 2014, Proceedings of ASME Turbo Expo 2014: Turbine Technical Conference and Exposition, Düsseldorf, Germany.
[6] Reitz, R. D., “Modeling Atomization Processes in High-Pressure Vaporizing Sprays”, 1987, Atomisation and Spray Technology, vol. 3, pp. 309–337.
[7] No, S.Y. “A review on empirical correlations for jet/spray trajectory of liquid jet in uniform cross flow”, 2015, Int. J. Spray Combust. Dynamics, 7,pp. 283-314
[8] Schmehl, R., Klose, G., Maier, G. and Wittig, S. “Efficient Numerical Calculation of Evaporating Sprays in Combustion Chamber Flows”, 1998, Proc. Symposium of the Applied Vehicle Technology Panel on Gas Turbine Engine Combustion, Emissions and Alternative Fuels, Lisbon, Portugal, pp. 51.1–51.13.
[9] Menter, F., “Stress-Blended Eddy Simulation (SBES) - A New Paradigm in Hybrid RANS-LES Modeling.” In: Hoarau Y., Peng SH., Schwamborn D., Revell A. (eds) Progress in Hybrid RANS-LES Modelling. HRLM 2016. Notes on Numerical Fluid Mechanics and Multidisciplinary Design, vol 137. Springer, Cham (2018)
[10] Wu, P., Kirkendall, K. A., Fuller, R. P., Nejad. A. S., “Spray Structures of Liquid Jets Atomized in Subsonic Crossflows”, 1998 Journal of Propulsion and Power 14:2, 173-182
[11] ANSYS® Release 2019 R1, Help System, Fluent User’s Guide, ANSYS, Inc.